Earth Planet. Sci. Lett. 643 (2024) 118825

Contents lists available at ScienceDirect

Earth and Planetary Science Letters

journal homepage: www.elsevier.com/locate/epsl

Vanadium isotope fractionation during plutonic differentiation and implications for the isotopic composition of the upper continental crust

Madeleine A. Stow [a], Julie Prytulak [a,*], Madeleine C.S. Humphreys [a], Samantha J. Hammond [b], Geoffrey M. Nowell [a]

[a] Department of Earth Sciences, Durham University, Durham DH1 3LE, UK
[b] School of Environment, Earth and Ecosystem Sciences, The Open University, Walton Hall, Milton Keynes MK7 6AA, UK

ARTICLE INFO

Edited by: Dr. F. Moynier

Keywords:
Vanadium isotopes
Granites
Magmatic differentiation
Continental crust

ABSTRACT

The analysis of emerging stable isotopic systems in clastic sedimentary rocks is increasingly used to determine the average composition of the upper continental crust through geological time. Any temporal variations can then be linked to global-scale processes such as the oxygenation of the atmosphere or onset of plate tectonics. Given that clastic sediments are ultimately eroded from the upper continental crust, knowledge of the potential isotopic variability in the plutonic rocks which make up the crust is vital for interpreting these sedimentary records.

Here we focus on the multi-valent transition metal element vanadium (V) and present the first investigation of the V isotopic composition of an upper crustal granitic pluton and its mineral separates. We use well-characterised samples from the calc-alkaline Boggy Plain Zoned Pluton, Australia. Whole rock samples and mineral separates show increases in $\delta^{51}V$ during magmatic differentiation, similar to what has been documented for extrusive differentiation suites. However, whole rock $\delta^{51}V$ is scattered, reflecting variations in the modal mineralogy and demonstrating the typical heterogeneity generated when dealing with coarse grained igneous rocks. In contrast, mineral separates show well-defined trends in $\delta^{51}V$, where mineral-melt fractionation factors are largely controlled by bonding environment rather than direct redox variations. We interpret the increase in $\delta^{51}V$ during magmatic differentiation to be driven by crystallisation of isotopically light magnetite, biotite and hornblende, in contrast with previous interpretations from extrusive lavas that oxide crystallisation alone is the main driver of V isotopic fractionation.

The overall range of whole rock samples and their mineral separates is > 0.6 ‰ within this single plutonic body. The range highlights that the upper continental crust can have extremely heterogeneous V isotopic composition over small geographic areas. This detailed examination of V isotopes in a simple system may shed light on the discrepancy between interpretations of the timing of felsic crust formation derived from the V and Ti isotopic compositions of glacial diamictites.

1. Introduction

Vanadium (V) is a moderately incompatible trace element which can exist in a variety of bonding environments and oxidation states. These characteristics give rise to analytically significant V stable isotope fractionation in terrestrial environments. The first procedure capable of generating precise and accurate V isotope measurements was published in 2011 (Nielsen et al., 2011; Prytulak et al., 2011). Vanadium isotopes have subsequently been applied to diverse problems such as investigating magmatic processes and physical parameters such as oxygen fugacity (e.g. Prytulak et al., 2013, 2016; Sossi et al., 2018; Wu et al., 2018; Qi et al., 2019; Ding et al., 2020; Novella et al., 2020; Stow et al., 2023), identifying the onset of subduction and formation of a felsic crust (Tian et al., 2023), development as an oceanic palaeoredox tracer (e.g. Schuth et al., 2019; Wu et al., 2020; Fan et al., 2021; Wei et al., 2023), and fingerprinting the sources of anthropogenic pollution (Huang et al., 2021).

The above applications all require an understanding of the isotopic mass balance of V between the main terrestrial reservoirs. To date, there has been no systematic investigation of the V isotopic composition of the

* Corresponding author.
E-mail address: julie.prytulak@durham.ac.uk (J. Prytulak).

https://doi.org/10.1016/j.epsl.2024.118825
Received 11 January 2024; Received in revised form 28 April 2024; Accepted 1 June 2024
Available online 22 July 2024

intermediate to felsic intrusive rocks which make up the majority of the upper continental crust, despite the fact that the upper crust is a significant V reservoir (V ~ 100 μg/g; Rudnick and Gao, 2014; Huang et al., 2015; Tian et al., 2023). The weathering of upper crustal rocks and transport of this material by rivers is the major source of V to the oceans (Shiller and Mao, 2000; Schuth et al., 2019). Additionally, physical erosion of the upper crust forms clastic sedimentary deposits, which have been analyzed to determine average crustal V isotopic composition through time (Tian et al., 2023). However, there are uncertainties with using clastic sediments to calculate average crustal compositions due to the effects of preferential weathering and hydrodynamic sorting (Klaver et al., 2021). Therefore, an understanding of the V isotopic composition of typical upper crustal rocks and their minerals is necessary to aid interpretations of complementary sedimentary records.

Vanadium has two isotopes, ^{50}V and ^{51}V, with natural abundances of 0.24% and 99.76% respectively. Vanadium isotopic compositions are reported in delta notation relative to the AA standard: $\delta^{51}V = [(^{51}V/^{50}V)_{sample}/(^{51}V/^{50}V)_{AA} - 1] \times 10^3$. Most previous $\delta^{51}V$ work on crustal rocks has focused on 'whole rock' (WR) samples from sequences of extrusive lavas (Prytulak et al., 2013; 2016; Wu et al., 2018; Qi et al., 2019; Novella et al., 2020; Ding et al., 2020; Stow et al., 2023). Vanadium isotopic fractionation is observed during fractional crystallisation, with increases in $\delta^{51}V$ of up to 2 ‰ in lavas from Hekla, Iceland, and Anatahan, Mariana arc, volcanoes (Prytulak et al., 2016). Lavas from Kilauea Iki, Hawaii, also show an increase in $\delta^{51}V$ of around 0.5 ‰ during magmatic differentiation (Ding et al., 2020).

Increases in WR $\delta^{51}V$ have been attributed to removal of isotopically light Fe-Ti oxides such as magnetite (e.g. Prytulak et al., 2016; Sossi et al., 2018; Ding et al., 2020). Vanadium is highly compatible in magnetite (Toplis and Corgne, 2002), and is most likely hosted as octahedrally co-ordinated V^{3+} (O'Neill and Navrotsky, 1984). Given that V is found in lower co-ordination in silicate melts (Giuli et al., 2004; Sutton et al., 2005; Righter et al., 2006), magnetite is theoretically predicted to be isotopically lighter than the melt from which it crystallises. The experimental study of Sossi et al. (2018) confirmed that magnetite is isotopically lighter than coexisting melt, and demonstrated that the V isotope fractionation between magnetite and melt ($\Delta^{51}V_{mag\text{-}melt}$) increases with increasing magmatic fO_2. Variations in the magnitude and timing of $\delta^{51}V$ increase during magmatic differentiation are theoretically attributed to variation in the chemistry of Fe-Ti oxides and the timing of oxide saturation (Ding et al., 2020). However, these hypotheses have not yet been tested via natural mineral separates or linked to differences in V bonding environment and redox state between mineral phases. The implication is that Fe-Ti oxides, which host the majority of V in the system, potentially have extremely variable $\delta^{51}V$ in different settings, which would impact the average $\delta^{51}V$ crustal composition.

Our understanding of V isotopes in extrusive lavas may not be directly applicable to the V isotopic composition of the continental crust. It is unknown how V isotopes behave in intrusive settings which have slowly crystallised over a large temperature range. For example, V isotopes could potentially be fractionated during low temperature oxy-exsolution of Fe-Ti oxides (e.g. Frost and Lindsley, 1991). In addition, it is not known whether felsic intrusive rocks will show similarly high $\delta^{51}V$ values as evolved lavas, given that plutonic rocks may be composed of both crystals and trapped interstitial melt, and thus whole rock compositions of coarse-grained rocks are not directly analogous to compositions of a comparatively crystal-poor evolving extrusive melt (e.g. Chappell and Wyborn, 2004).

Therefore, an investigation of intrusive rocks and their mineral separates is required for a more complete understanding of crustal V isotopic composition. Here, we present the first V isotope measurements of whole rock samples and their V-rich mineral separates (biotite, hornblende and magnetite) from a cogenetic calc-alkaline pluton representative of typical upper continental crust. We determine the range in $\delta^{51}V$ and investigate the controls on V isotopic fractionation. We then discuss implications for the V isotopic composition of the upper continental crust, and the use of clastic sediments to infer temporal variations in crustal composition.

2. Geological background

Whole rock samples and mineral separates are from the concentrically zoned Boggy Plain Zoned Pluton (BPZP), SE Australia (Fig. 1). The BPZP has several characteristics that make it an ideal case study to investigate the behaviour of V isotopes in an intrusive setting. The BPZP is well characterised chemically and petrographically, and is a relatively simple plutonic body where major and trace element variations have been interpreted in the context of approximately closed system fractional crystallisation of a single body of calc-alkaline magma (Wyborn, 1983; Wyborn et al., 1987; Hoskin et al., 2000, Wyborn et al., 2001; Ickert et al., 2011; Park et al., 2013; Stow et al., 2022). As discussed in Wyborn (1983) and Stow et al. (2022), mafic cumulate samples with WR MgO >4.5 wt.% display scattered concentrations of major and trace elements, reflecting variable proportions of cumulus minerals. Below 4.5 wt.% WR MgO, samples typically display smooth variations in concentration, controlled by the fractionating mineral assemblage. Whole rock V concentrations (Fig. 1) follow this framework, with scattered WR V above 4.5 wt.% WR MgO, and a smooth decrease in WR V below 4.5 wt.% WR MgO, driven by the crystallisation of titanomagnetite (herein referred to as magnetite), biotite and hornblende as the fractionating mineral assemblage. The samples in this study are the same as used for Fe and Zn isotopic analyses in Stow et al. (2022).

3. Methods

3.1. Vanadium separation

Vanadium separation and isotopic analysis was conducted in the Arthur Holmes Isotope Geology Laboratory, Durham University. Whole rock powders were ground using a Fritsch Pulverisette 0 agate mortar and ball. Biotite and hornblende separates were hand-picked under binocular microscope from a 125 – 250 μm size fraction, avoiding crystals with obvious inclusions or alteration features. The magnetite separates were initially separated from silicate material using a hand magnet, and then further hand-picked under binocular microscope. Mineral separates were ground into powders by hand using an agate pestle and mortar, which was cleaned with low Fe quartz sand between each sample. To make at least three V isotopic measurements, approximately 1.5 μg total V is required. Biotite and hornblende contain 200 – 800 μg/g V (Wyborn, 1983), and magnetite separates contain 1000 – 5000 μg/g V (Section 4.2), so approximately 20 – 30 mg material was picked and digested. For the whole rock samples (14 – 292 μg/g V; Wyborn, 1983), between 50 – 70 mg of powder was digested.

Powders and silicate mineral separates were digested in a 3:1 mixture of Teflon distilled (TD) 29 M HF and TD 16 M HNO_3 in sealed Teflon beakers on a hotplate at 160 °C for at least 48 h. The magnetite separates were digested in 5 ml TD 6 M HCl on a hotplate at 120 °C for 48 h. This is because after hand-picking, magnetite grains sometimes contained small silicate inclusions, or silicate material attached to the margins of grains. Although silicate material typically contains an order of magnitude lower V concentration than magnetite (see mineral separate V concentrations above), silicate minerals may have distinct V isotopic compositions. Using 6 M HCl permits full digestion of the oxide grains and the insoluble silicates are subsequently separated by centrifugation. Samples were evaporated at 120 °C then taken up in 1 ml TD 6 M HCl for column chromatography. A 20 μl aliquot was taken from the magnetite samples at this stage for trace element analysis.

Vanadium chemical separation follows the procedure outlined in Nielsen et al. (2011), modified by Wu et al. (2016). The underlying principle is that V^{5+} forms anionic V-peroxide complexes with hydrogen peroxide (H_2O_2) in mildly acidic solutions, which will partition strongly

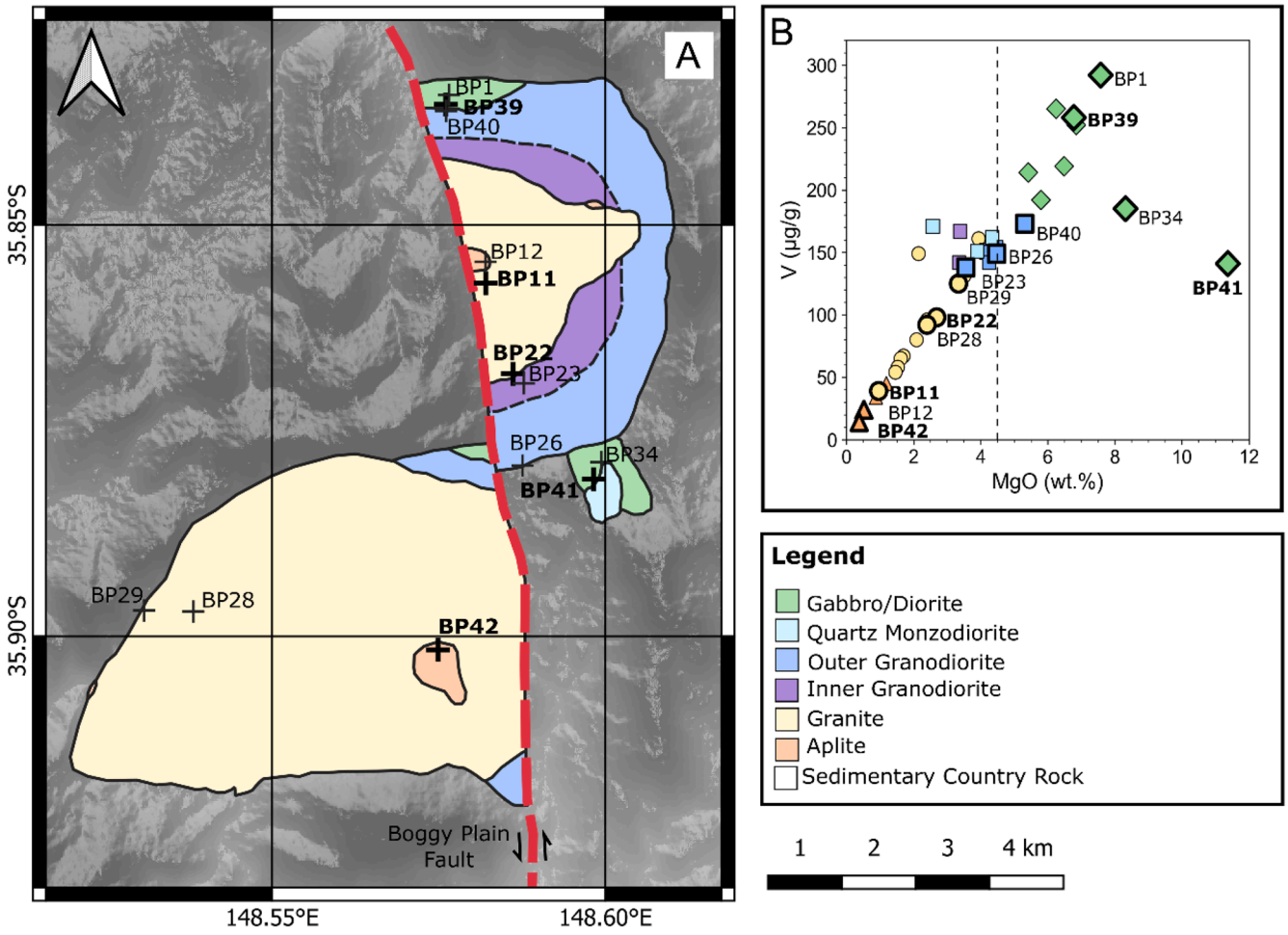

Fig. 1. (A) Geological Map of the Boggy Plain Zoned Pluton. Sample localities are shown by crosses. Mineral separates were picked from the samples highlighted in bold. (B) Plot of whole rock MgO and V concentrations, data from Wyborn (1983). Samples with bold outlines are those analysed in this study. The vertical dashed line at 4.5 wt.% MgO approximates the separation of liquids from cumulate rocks (see text).

onto anion exchange resins such as AG1-X8. However, Fe and Ti must be removed before H_2O_2 can be used, because Fe and Ti catalyse the dissociation of H_2O_2 to water and oxygen, causing loss of V because V-peroxide complexes can no longer form (Nielsen et al., 2011). Therefore, column 1 removes Fe and column 2 removes Ti, in preparation for column 3, where V is complexed with H_2O_2 to separate it from Cr and other matrix elements. The minor ^{50}V isotope has direct isobaric interferences from ^{50}Cr and ^{50}Ti. Therefore, near quantitative separation of V from Ti and Cr is required. Columns 4 and 5, from Nielsen et al. (2011) are 'clean-up' columns designed to remove trace Cr and Ti that can be repeated as necessary depending on sample matrix.

3.2. Vanadium isotopic analysis

Vanadium isotopic compositions were measured on a Neptune MC-ICP-MS, following the protocol outlined in Wu et al. (2016). Measurements were made in medium resolution mode ($m/\Delta m$ = 6000–8000), allowing V to be resolved from isobaric interferences on the shoulder on the low mass side of the peak. Masses ^{48}Ti, ^{49}Ti, ^{50}V, ^{51}V, ^{52}Cr and ^{53}Cr were measured in cups L4, L2, L1, C, H1 and H3 respectively. A $10^{10}\Omega$ resistor was connected to the centre cup to measure signals >50 V on ^{51}V. This allows samples to be measured at higher concentrations, thereby increasing the signal on the minor ^{50}V isotope (the natural $^{51}V/^{50}V$ ratio is ~ 420).

Standards and samples were run at concentrations of 1 ppm V. The sample introduction system consisted of a PFA Concentric Flow nebuliser coupled to an Aridus 3 Desolvating Nebuliser System. Typical sensitivity was >100 V/ppm on ^{51}V. Mass bias and instrument drift was corrected by standard sample bracketing with the AA standard (Nielsen et al., 2011). The BDH V solution (Nielsen et al., 2011) was measured throughout analytical sessions to assess machine precision and accuracy. The long-term average was $\delta^{51}V = -1.23 \pm 0.10$ ‰ (2SD, n = 397), which is within error of values from other studies (e.g. Nielsen et al., 2011; Wu et al., 2016; Schuth et al., 2019; Wu et al., 2019). USGS Reference Materials were processed with each batch of chemistry (Table 1), and $\delta^{51}V$ values agree with previously published values (e.g. Prytulak et al., 2011; Wu et al., 2016; Qi et al., 2019).

^{48}Ti, ^{49}Ti, ^{52}Cr and ^{53}Cr were used to correct for interferences of ^{50}Ti and ^{50}Cr on ^{50}V, using the exponential law ($R_T = R_M \times (m_1/m_2)^{\beta}$. Two BDH solutions were doped with 100 ppb Ti and Cr respectively, and measured in every sequence in order to determine β values for Cr and Ti, after Wu et al. (2016).

3.3. Magnetite trace element concentrations

Variation in the chemistry of oxide minerals has been shown to influence the isotopic compositions of Fe (Rabin et al., 2021) and Ti (Hoare et al., 2022). Therefore, it is important to evaluate the composition of the BPZP magnetite when interpreting V isotopic data, because magnetite is a major V host. However, a challenge with chemical analysis of Fe-Ti oxide minerals in intrusive rocks is that oxides are susceptible to subsolidus re-equilibration during slow cooling. In

Table 1
Vanadium isotopic composition of BPZP whole rock powders. Isotopic compositions given relative to the AA standard. WR SiO_2, MgO and V data from Wyborn (1983). Errors are given as 2 standard deviations of the mean of at least 3 measurements of the sample. When fewer than 3 measurements were made, errors are reported as 2SE (*). Note that for sample BP40, two separate whole rock powders made from the same sample were analysed ($). The synthetic magnetite powder is an in-house standard used due to its similar matrix to real oxide mineral separates (+).

Sample	Rock Type	WR SiO_2 (wt. %)	WR MgO (wt. %)	WR V (μg/g)	$\delta^{51}V_{AA}$ (‰)	2SD	n
BP34	Diorite	53.49	8.32	185	−0.94	0.03	3
BP1	Diorite	52.22	7.58	292	−0.98	0.06	3
BP39	Diorite	52.24	6.78	258	−1.04	0.06	3
BP40	Granodiorite	58.88	5.32	173	−0.85	0.11	3
	Replicate Digestion$				−1.15	0.04	3
BP26	Granodiorite	61.16	4.48	149	−0.72	0.04	3
BP23	Granodiorite	61.97	3.56	138	−0.60	0.07	3
	Replicate digestion				−0.59	0.08	3
BP29	Granite	63.12	3.34	125	−0.90	0.10	4
BP22	Granite	65.43	2.69	98	−0.85	0.06	3
BP28	Granite	66.40	2.40	92	−0.79	0.06	3
	Replicate Digestion				−0.67	0.01	3
BP11	Granite	72.37	0.96	39	−0.81	0.07	3
BP12	Aplite	73.07	0.52	24	−0.71	0.04*	1
	Replicate digestion				−0.73	0.09	3
BP42	Aplite	74.80	0.38	14	−0.56	0.06	3
USGS Reference Materials							
GSP-2					−0.58	0.06	4
BIR-1a					−0.90	0.04	5
BIR-1a					−0.98	0.06	5
Other in-house reference materials							
Synthetic Magnetite Powder+					−0.96	0.07	3
Synthetic Magnetite Powder+					−0.85	0.06	5

magnetite, this results in low temperature oxyexsolution of ilmenite as lamellae or granules (Frost and Lindsley, 1991). Exsolved domains and host may have distinct isotopic compositions, as has been reported previously for both Fe (e.g. Dziony et al., 2014; Chen et al., 2014; Cao et al., 2019) and Mg isotopes (Chen et al., 2021). It is not currently known what effect exsolution may have on V isotopes.

Trace element concentrations of the magnetite mineral separates were obtained from the same aliquots used for isotopic measurements. Approximately 10–20 mg of magnetite mineral separates were hand-picked and digested in 5 ml TD 6 M HCl. A 20 μl aliquot was taken from the sample dissolved in 1 ml TD 6 M HCl before it was loaded onto the first column. By sampling a large number of whole crystals, this gives the average 'bulk' composition of the magnetite before any exsolution occurred. This bulk analysis approach was preferred to in-situ analysis (e.g. by LA-ICP-MS) because it allows magnetite grains and any ilmenite that may have exsolved during cooling to be sampled together. Magnetite separates were digested in TD 6 M HCl to minimise digestion of any silicate inclusions. Hence, the exact mass of magnetite digested is not known and the trace element concentrations will be minimum values.

Trace element analysis of the oxide mineral bulk separates was conducted at the Open University, UK, using an Agilent 8800 ICP-QQQ-MS inductively coupled plasma mass spectrometer. Samples were evaporated and taken up in 2% HNO_3 for a 4000-fold dilution. These dilutions were aspirated using a quartz microflow nebuliser with uptake rate 500 μl/min. The Agilent 8800 contains two quadrupoles and a collision/reaction cell (Octopole Reaction System; ORS) which can be operated in three configurations: 'no gas', 'He gas' or 'O_2 mass shift'. Most elements were measured in 'no gas' mode, except for the Rare Earth Elements (La to Lu) where O_2 gas was used to shift the mass by 16. The first quadrupole controls the masses which enter the ORS, and the second quadrupole is used in either mass-shift or on-mass mode depending on whether a gas is used in the reaction cell (e.g. Wei et al., 2017; Brett et al., 2018). Calibration standards of known concentration were run at the start of each measurement session. An in-house synthetic magnetite powder *Synth. Mag.* (>96.8 wt. % Fe_3O_4) from Inoxia Ltd was measured before and after the BPZP magnetite samples. Errors are reported as the within run RSD of each individual analysis. For the first-row transition metals which were the focus of this work, RSDs were typically <5%.

4. Results

4.1. Vanadium isotopic compositions of whole rock and mineral separates

The V isotopic composition of the whole rock powders and mineral separates are shown in Tables 1 and 2. The data are the first V isotopic measurements reported thus far for silicate and oxide minerals from granites.

4.1.1. Whole Rock Powders

There is an increase in whole rock $\delta^{51}V_{AA}$ from −1.15 ± 0.04 ‰ (2SD) to −0.56 ± 0.06 ‰ (2SD), with decreasing WR MgO and increasing WR SiO_2 content (Fig. 2), although the data are scattered. For several samples, the isotopic composition of a separate digestion of the same powder was measured. For samples BP12 and BP23, the $\delta^{51}V$ values of the two digestions agree within error. However, the $\delta^{51}V$ values for the two digestions of BP28 do not reproduce (indicated on Fig. 2). For BP40, two separate powders were made from the same initial whole rock sample, and these display distinct $\delta^{51}V$ values. Replicate digestions of mineral separates were also made, which involved picking new mineral grains from the remaining sample crushate and making a new powder. The $\delta^{51}V$ values for the replicate digestions of mineral separates all reproduce within error (Table 2). This highlights the potential issue of powder heterogeneity in whole rock powders from coarse grained granitic rocks, especially for elements like V which can be concentrated in low abundance accessory phases such as magnetite.

Table 2
Vanadium isotopic composition of BPZP mineral separates. Isotopic compositions given relative to the AA standard. I and P denote whether the mineral is present as an interstitial phase (I) or primocryst (P). Errors are given as 2 standard deviations of the mean of at least 3 measurements of the sample. When fewer than 3 measurements were made, errors are reported as 2SE (*). V concentration data and modal abundances for the mineral separates are given in Table S-3.

Sample	Mineral Phase	Texture	$\delta^{51}V_{AA}$ (‰)	2SD	n
BP41	Biotite	I	−0.88	0.11	3
BP39	Orthopyroxene	P	−0.80	0.05*	2
	Biotite	I	−0.92	0.05*	2
	Hornblende	I	−1.09	0.11	3
	Magnetite	I	−1.26	0.12	3
BP40	Magnetite	P	−1.06	0.02	3
BP22	Biotite	P	−0.71	0.05*	2
	Hornblende	P	−0.81	0.05*	2
	Magnetite	P	−0.81	0.05	3
BP11	Biotite	P	−0.66	0.09	3
	Biotite (Replicate)	P	−0.74	0.06	4
	Hornblende	P	−0.79	0.04*	2
	Magnetite	P	−0.65	0.03	3
BP42	Biotite	P	−0.47	0.07	3
	Magnetite	P	−0.58	0.11	3
	Magnetite (Replicate)	P	−0.59	0.06	5

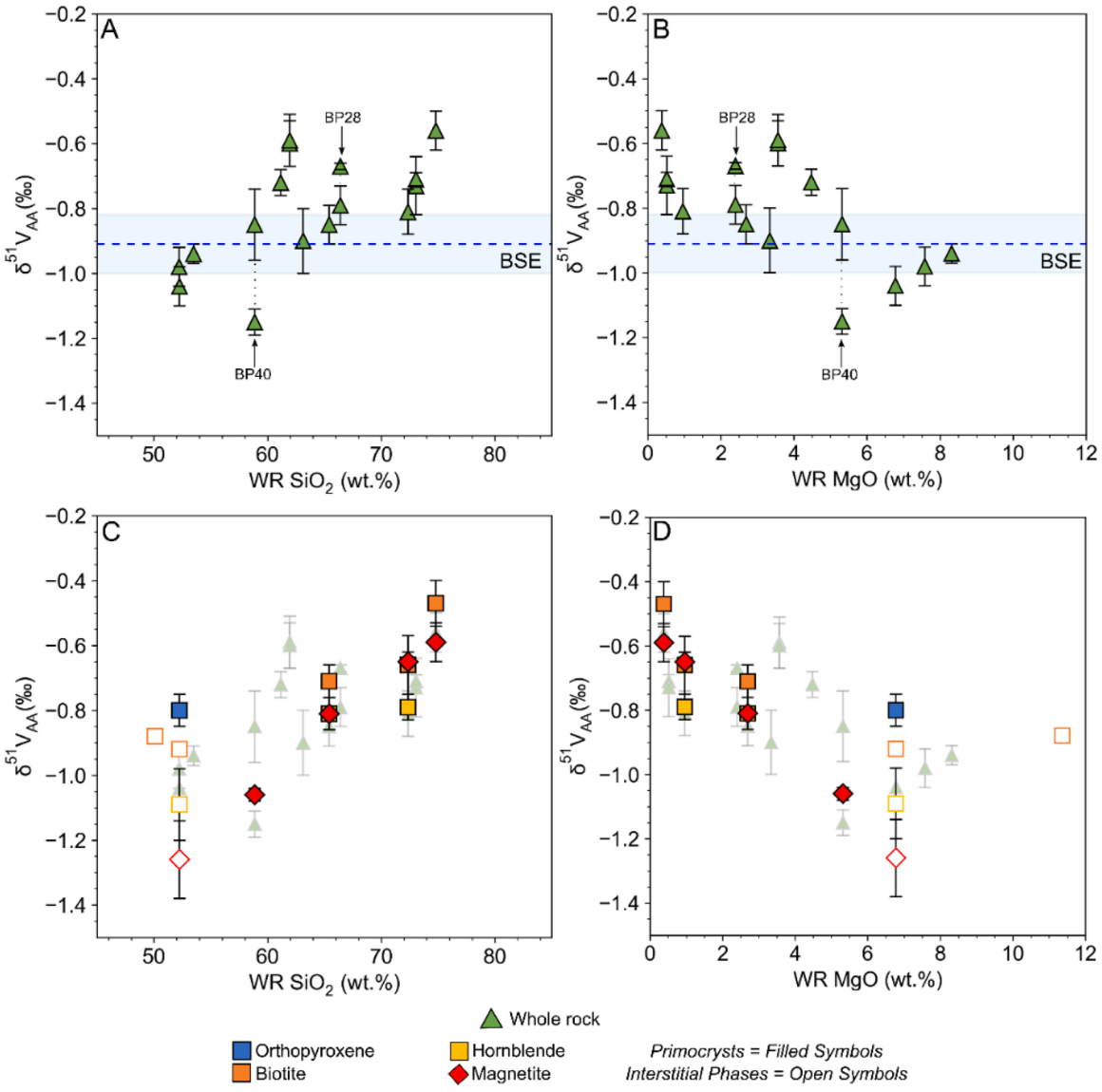

Fig. 2. Variation in $\delta^{51}V$ for WR samples (A and B) and mineral separates (C and D) with WR MgO and SiO_2 content. WR and mineral separates both show an increase in $\delta^{51}V$ with increasing WR SiO_2 and decreasing WR MgO, driven by fractional crystallisation. The WR data is more scattered than the mineral separate data, likely due to the inherent heterogeneity of coarse-grained samples. Whole rock SiO_2 and MgO data are from Wyborn (1983). The blue shaded area is the estimate for the BSE from Qi et al. (2019) of -0.91 ± 0.09 ‰. (2SD, $n = 18$). Errors are plotted as 2SD of at least 3 individual measurements of each sample. When < 3 analyses were made, errors are reported as the internal 2SE of an individual measurement. Samples BP40 and BP28 are labelled. Replicate digestions of these samples did not reproduce, see Table 1 and text for more details.

4.1.2. Mineral Separates and mineral-mineral isotope fractionation factors

The BPZP samples are coarse grained intrusive rocks, composed both of euhedral primocryst phases and interstitial phases with irregular, anhedral morphologies (Figure S-1). The primocryst phases are assumed to have crystallised from the main magma body, and are likely in chemical equilibrium with other primocrysts. The interstitial phases crystallised from melt trapped in isolated sites between the primocrysts, and thus interstitial phases are not necessarily in chemical equilibrium with the primocrysts (Wyborn, 1983; Stow et al., 2022). These petrographic observations must be considered when interpreting isotopic trends and inter-mineral fractionation factors.

Magnetite, biotite and hornblende mineral separates show trends of increasing $\delta^{51}V$ with decreasing WR MgO and increasing WR SiO_2 (Fig. 2). These variations are well-defined compared to the WR trends. Primocryst biotite and magnetite from the same sample have $\delta^{51}V$ values within error, whilst primocryst biotite is approximately 0.1 ‰ higher than primocryst hornblende from the same sample.

There are several lines of evidence which support the interpretation that the primocryst phases achieved inter-mineral V isotopic equilibrium. Firstly, primocryst phases show regular, euhedral morphologies, indicative of unconfined crystallisation from the main magma body (Wyborn, 1983; Stow et al., 2022). Replicate analyses of additional hand-picked aliquots of the mineral separates give reproducible $\delta^{51}V$ values (Table 2). The same mineral separates display inter-mineral Fe isotope fractionation factors which agree with theoretical equilibrium values (Stow et al., 2022). Together this evidence supports the attainment of inter-mineral V isotopic equilibrium.

Inter-mineral fractionation factors ($\Delta^{51}V_{mag\text{-}bt}$ and $\Delta^{51}V_{bt\text{-}hbd}$) for primocryst phases show no relationship with temperature, or parameters of differentiation (Fig. 3; filled symbols). Note that the apparent trend of $\Delta^{51}V_{mag\text{-}bt}$ with WR MgO, WR SiO_2 and temperature is exaggerated by the $\Delta^{51}V_{mag\text{-}bt}$ value for interstitial biotite and magnetite in sample BP39, which likely did not crystallise in isotopic equilibrium based on crystal textures observed in thin section (Stow et al., 2022). If

this value is ignored, primocryst $\Delta^{51}V_{mag\text{-}bt}$ values are all approximately zero.

4.2. Transition metal concentrations of magnetite separates

The V and Ti concentrations of the magnetite mineral separates are shown in Fig. 4. All other elements with concentrations above detection levels are reported in Table S-1. Concentrations of V and Ti in magnetite decrease with WR MgO content, a proxy for degree of differentiation. The data fall on the same general trend as values measured by LA-ICP-MS by Park et al. (2013) in a different set of samples from the BPZP.

A key motivation for analysing the trace element composition of the magnetite mineral separates processed for V isotope ratio measurements was to measure the Ti content of the bulk oxide separates to assess if we were sampling magnetite and/or ilmenite. Petrographic observations suggest that magnetite is the dominant Fe-Ti oxide in the BPZP during differentiation (Wyborn, 1983). All magnetite samples have very low Ti content (<0.5 wt.% TiO_2 with the exception of the interstitial magnetite from BP39 which has 4.5 wt.% TiO_2). Together with a lack of visible exsolution lamellae under reflected light in all samples (see Fig 4. in Stow et al., 2022), this suggests that the oxides measured in this study are magnetite, which has undergone little low T re-equilibration, and V isotope data can be interpreted within this context.

5. Discussion

In this section, we discuss the causes of the variation in $\delta^{51}V$ in whole rock powders and mineral separates from the BPZP, and the implications for our understanding of the V isotopic composition of the continental crust.

5.1. Caveats to bulk sampling of coarse-grained material for isotope analyses

Although the BPZP WR samples display an increase in $\delta^{51}V$ during differentiation, the values are highly scattered compared to trends observed in extrusive lava suites (Prytulak et al., 2016; Wu et al., 2018; Ding et al., 2020). There is the potential that some scatter is driven by variation in the magma source. Using Nd-Hf-O isotopes, Ickert (2010) demonstrated that the diorite and granodiorite bodies are formed by the melting and differentiation of different sources than the main granitic body of the pluton. However, given that all mafic volcanic rocks measured to date fall within the range $\delta^{51}V = -0.8$ ‰ to -1.0 ‰ (Prytulak et al., 2013, 2016; Wu et al., 2018; Qi et al., 2019; Ding et al., 2020; Novella et al., 2020; Stow et al., 2023), any variation in source $\delta^{51}V$ is likely minor (maximum ~0.2 ‰) and cannot account for the scatter in WR $\delta^{51}V$ in samples from the main granite body.

Modal mineralogy may have a key role to play in generating WR $\delta^{51}V$ variability. It is important to consider the difference in whole rock samples from extrusive and intrusive settings. Whereas a rapidly quenched, phenocryst poor lava records the composition of the melt from which it crystallised, intrusive whole rock samples represent variable proportions of crystals and melt that may not have coexisted at equilibrium (e.g. Chappell and Wyborn, 2004). It is also likely that these crystals have been partially separated from coexisting melt by processes such as crystal settling and/or compaction (e.g. Bachmann and Bergantz, 2004; Holness, 2018). This is especially important for trace elements like V, which are concentrated in certain dense mineral phases. Decimetre scale modal layering is observed in samples in the field (Wyborn, 1983), and thus variations in modal mineralogy at this scale could influence the isotopic composition of different powders made from the same hand sample.

Considering that the constituent mineral separates within single samples can span a range in $\delta^{51}V$ from 0.1 ‰ to 0.4 ‰ (Fig. 2), variation in modal abundance could have a sizable influence on WR isotopic composition. This process is most sensitive to the modal abundance of magnetite which has the highest V concentration. We use mass balance calculations to demonstrate how realistic variations in the modal proportion of magnetite may influence WR $\delta^{51}V$. By varying the modal abundance of magnetite between 0.5% and 4%, the resultant WR $\delta^{51}V$ varies by up to 0.3 ‰ (see Supplementary Information). Therefore, variation in mineral abundance on the hand-sample scale can justify why replicate digestions of the BP28 WR powder do not reproduce.

For sample BP40, two separate WR powders were made from the same initial sample block to investigate the possible control of the decimetre scale modal layering observed in the field on WR $\delta^{51}V$ (see Supplementary Information for more detail). The two powders have distinct $\delta^{51}V$ values, demonstrating that variations in modal mineralogy at the hand-sample scale also exert an important control on WR $\delta^{51}V$. This highlights the caveats which must be considered when interpreting WR isotopic trends in coarse grained intrusive rocks, and emphasises the importance of the petrographic examination of samples.

5.2. Why does $\delta^{51}V$ increase during magmatic differentiation?

Previous studies have attributed increases in WR $\delta^{51}V$ in extrusive lavas to crystallisation and removal of isotopically light minerals, which drives the residual magma to a heavier isotopic composition (Prytulak et al., 2016; Ding et al., 2020). Prytulak et al. (2016) proposed that the most likely phase driving this increase was (titano)magnetite, because V is highly compatible in magnetite (e.g. Toplis and Corgne, 2002). Magnetite contains predominantly trivalent V in octahedral coordination (O'Neill and Navrotsky, 1984), whereas silicate melt contains IV- and V-fold V at higher redox state (Giuli et al., 2004; Sutton et al., 2005; Righter et al., 2006). Therefore, magnetite is theoretically predicted to be isotopically lighter than coexisting melt at equilibrium (e.g. Wu et al., 2015). Isotopically light magnetite was supported by the experimental study of Sossi et al. (2018) who determined negative $\Delta^{51}V_{mag\text{-}melt}$ values ranging from -0.63 ± 0.09 ‰ to -0.92 ± 0.11 ‰. Recent work has also indicated that oxide mineralogy will determine the extent of increase in WR $\delta^{51}V$. Comparisons of Fe-V-Ti isotopes in lavas from Kilauea Iki, Hekla and Anatahan hint that magnetite, Ti-rich ulvöspinel and ilmenite may have distinct $\Delta^{51}V_{min\text{-}melt}$ values (Ding et al., 2020), although this has not been tested directly using mineral separates.

In contrast to previous studies on extrusive lavas, we find that magnetite is not the dominant V bearing phase in the BPZP. Biotite and hornblende contain between 200 – 800 μg/g V (Wyborn, 1983), and both minerals have modal abundances of approximately 5–15 % in samples spanning the differentiation sequence. Therefore, although the magnetite in the BPZP has the highest absolute V concentration (~1000 – 8000 μg/g V; Fig. 4), mass balance calculations show that the silicate phases can account for 40–65 % of the V budget in individual samples, and therefore exert an important control on the V isotopic composition of the evolving melt. Biotite and hornblende predominantly host V^{3+} in VI-fold coordination, substituting for VI-fold Fe^{3+} which has a similar ionic radius (Shannon et al., 1976). Therefore, silicate minerals should theoretically also be isotopically lighter than coexisting melt at equilibrium. The combined fractional crystallisation of isotopically light biotite, hornblende and magnetite therefore drives the increase in magma $\delta^{51}V$ in the BPZP.

The BPZP was chosen for this study because it is a relatively simple intrusive suite, where chemical trends in the main granitic body of the pluton are largely driven by closed system fractional crystallisation. We use a Rayleigh fractionation model to quantify the bulk $\Delta^{51}V_{min\text{-}melt}$ required to drive the increase in WR $\delta^{51}V$ observed across the pluton. It must be noted that this type of calculation is not necessarily wholly appropriate for intrusive systems, because WR compositions may not be directly analogous to an evolving melt, and complete separation of crystals and melt may not occur in mush-dominated magmatic systems. In addition, we cannot rule out that other disequilibrium processes, for example diffusion and re-adsorption of crystals, occurring in long-lived crustal magma reservoirs before they are fully crystallised. However,

this approach allows us to compare the bulk $\Delta^{51}V_{min\text{-}melt}$ for the BPZP to previous studies, including other subduction-related volcanic rocks from the Southern Lesser Antilles and the Aleutians from Tian et al. (2023).

We focus on the granite body of the pluton (from WR MgO content of 3.34 wt.% onward) to minimise complications from the potential influence of different melt sources (e.g. Ickert, 2010). Using sample BP29 for the parental melt composition, a Rayleigh model demonstrates that a bulk $\Delta^{51}V_{min\text{-}melt}$ value between −0.05 ‰ to −0.10 ‰ is required to describe the $\delta^{51}V$ trends in the WR data (Fig. 5). Given the similar values of the primocrysts phases in individual samples, calculating a bulk $\Delta^{51}V_{min\text{-}melt}$ value rather than individual fractionation factors for the different mineral phases is appropriate in this case, and implies that $\Delta^{51}V_{bt\text{-}melt}$, $\Delta^{51}V_{hbd\text{-}melt}$ and $\Delta^{51}V_{mag\text{-}melt}$ are also approximately −0.05 ‰ to −0.10 ‰.

The bulk $\Delta^{51}V_{min\text{-}melt}$ for the BPZP (−0.05 ‰ to −0.10 ‰) is very similar to the bulk $\Delta^{51}V_{min\text{-}melt}$ of −0.11 ‰ which describes the $\delta^{51}V$ trends observed in the subduction-related volcanic rocks in Tian et al. (2023), which is unsurprising given that the suites have broadly similar chemistries and fractionating mineral assemblages. This similarity supports the interpretation that fractional crystallisation is the major control on the $\delta^{51}V$ variations in the BPZP, and suggests that other calc-alkaline magmas undergoing fractional crystallisation should display similar ranges in $\delta^{51}V$. The BPZP bulk $\Delta^{51}V_{min\text{-}melt}$ is also similar to that at Kilauea Iki (−0.15 ‰; Ding et al., 2020) despite this being a tholeiitic system. In contrast, the BPZP bulk mineral-melt fractionation factors are lower than the bulk $\Delta^{51}V_{min\text{-}melt}$ values of −0.4 ‰ to −0.5 ‰ proposed for the Hekla and Anatahan extrusive volcanic suites.

We suggest several reasons for the contrasting calculated bulk $\Delta^{51}V_{min\text{-}melt}$ in these suites. Firstly, Tian et al. (2023) proposed that primary magmas with Fe enrichment have enhanced magnetite crystallisation, causing the evolution of the magma to extremely high $\delta^{51}V$ of ~+1 ‰. The primary magmas at Hekla and Anatahan have Fe# ~70 (where Fe# = 100 x $FeO_T/(FeO_T + MgO)$), whereas the Kilauea Iki, Lesser Antilles and Aleutian lavas have Fe# <60 (Tian et al., 2023). The most mafic BPZP samples also have low Fe# (40–60), and thus this lack of extreme Fe enrichment and enhanced magnetite crystallisation may explain the lower bulk $\Delta^{51}V_{min\text{-}melt}$ values in the BPZP. In addition, the specific chemistry of the Fe-Ti oxides may also influence the magnitude of oxide-melt fractionation factors (Ding et al., 2020), although further investigations of mineral separates are required to test this hypothesis. Finally, to promote large bulk mineral-melt fractionation factors requires that the isotopically light mineral phase must be efficiently removed from the melt and the system must be closed to further input. However, this is unlikely in mush dominated magma reservoirs such as the BPZP where light phases may be re-dissolved in the melt, which would mute and lead to scatter the overall $\delta^{51}V$ trend. Further work is required to confirm whether these mineral-melt fractionation factors are truly representative. However, the BPZP data provide a useful baseline for the degree of V isotope fractionation expected in simple intrusive calc-alkaline systems, which is required for future work on more complex mush systems and the continental crust in general.

5.3. Controls on mineral-melt and inter-mineral V isotope fractionation factors

Biotite, hornblende and magnetite mineral separates show well defined trends of increasing $\delta^{51}V$ with decreasing WR MgO and increasing WR SiO_2 (Fig. 2). Fundamentally, at equilibrium, the V isotopic composition of the minerals depends on the isotopic composition of the melt from which they crystallise, and the isotopic fractionation factor ($\Delta^{51}V_{min\text{-}melt}$) between that mineral and the melt. Fractionation factors are controlled by variation in valence state and bonding environment between mineral and melt, and external factors including temperature and fO_2 (e.g. Schauble, 2004). In an intrusive system, there is no coexisting melt phase to analyse, so mineral-melt fractionation factors cannot be directly determined. Instead, variations in the magnitude of inter-mineral fractionation factors can be examined.

Primocryst biotite and magnetite have identical V isotopic composition in the same sample, and hornblende is approximately 0.1 ‰ lower than biotite (Fig. 3). This indicates that $\Delta^{51}V_{min\text{-}melt}$ and thus V-O bond strength is approximately equal for all three minerals. Assuming that magma temperature and fO_2 are constant in an individual sample, the similar $\Delta^{51}V_{min\text{-}melt}$ values imply that the oxidation state and bonding environment of V is similar in these minerals.

In biotite, hornblende and magnetite, most V substitutes as V^{3+} on octahedral sites, due to its high octahedral site preference energy (e.g. Sossi et al., 2018). The most likely substitution is $^{VI}V^{3+}$ (0.640 Å) for $^{VI}Fe^{3+}$ (0.645 Å) given their similar ionic radii (Shannon, 1976). The ^{VI}Fe-O (and hence ^{VI}V-O) bond lengths are similar in all phases (Redhammer and Roth, 2002; Sossi and O'Neill, 2017; Nie et al., 2021). Taken together, all three minerals appear to have similar bonding environments for V, so large inter-mineral fractionation factors are not expected, which is consistent with our observations.

There is still the potential that differences in the V^{4+}/V^{3+} ratio between mineral phases can influence isotopic composition. Although V^{3+} is the most compatible ion, the more oxidised V species can also be incorporated into minerals through direct or coupled substitutions which satisfy charge balance. For example, pure magnetite contains both V^{3+} and V^{4+} on VI-sites, with stoichiometry set to balance the constant Fe^{3+}/Fe^{2+} ratio through the substitution $Fe^{2+} + V^{4+} = Fe^{3+} + V^{3+}$ (O'Neill and Navrotsky, 1984). However, the V^{4+}/V^{3+} ratio would vary if other cations were present, for example if V^{4+} is able to substitute for Ti^{4+} (e.g. Toplis and Corgne, 2002). Based on bond valence theory, isotopically heavy V is predicted to concentrate in bonds containing V in a higher valence state, so minerals with higher V^{4+}/V^{3+} ratios would be isotopically heavier (e.g. Wu et al., 2015). It is unlikely that the partition coefficients for $V^{3+}$and V^{4+} would be the same in magnetite, biotite and hornblende due to their different chemical compositions which would lead to a difference in mineral V^{4+}/V^{3+}. However, given the identical isotopic compositions of biotite, hornblende and magnetite in the same sample, this would suggest that the overwhelming control on inter-mineral V fractionation factors is mineral bonding environment, for example bond length and co-ordination, rather than variation in valence state.

5.4. $\delta^{51}V$ of magnetite and relationship with melt fO_2

There is no coexisting melt phase to analyse in the BPZP, so it is not possible to give absolute $\Delta^{51}V_{min\text{-}melt}$ values for magnetite, biotite and hornblende. However, Sossi et al. (2018) determined the V isotope fractionation factor between pure magnetite and melt ($\Delta^{51}V_{mag\text{-}melt}$), to which our data can be compared.

Sossi et al. (2018) demonstrated that $\Delta^{51}V_{mag\text{-}melt}$ varies with melt fO_2, and hypothesised that the V isotopic composition of magnetite could potentially be a useful fO_2 indicator. The experiments were conducted over a fO_2 range of 6 log units (FMQ −1 to FMQ +5), which encompasses and exceeds typical fO_2 values of terrestrial magmas. The temperature (800 °C) and melt composition (hydrous haplogranite) are also geologically relevant to the crystallisation conditions of the BPZP (Sossi et al., 2018; Wyborn, 1983). Therefore, the BPZP samples provide an opportunity to investigate this hypothesis directly using the magnetite mineral separates.

In the BPZP, magnetite $\delta^{51}V$ shows a positive correlation with WR $Fe^{3+}/\Sigma Fe$ content with an R^2 value of 0.9962 (Fig. 6). This trend could, at first glance, be interpreted as the V isotopic composition of the minerals directly recording variations in magma fO_2 (i.e. heavier isotopic composition at more oxidising conditions). However, this mechanism is unlikely when we consider the details of the experimental work of Sossi et al. (2018). Quantitative determinations of oxygen fugacity are difficult for intrusive rocks like the BPZP, but estimates suggest initial magma fO_2 of approximately FMQ-1, and an increase of 1–2 log units during fractional crystallisation (Wyborn, 1983). For a fO_2 variation of 2

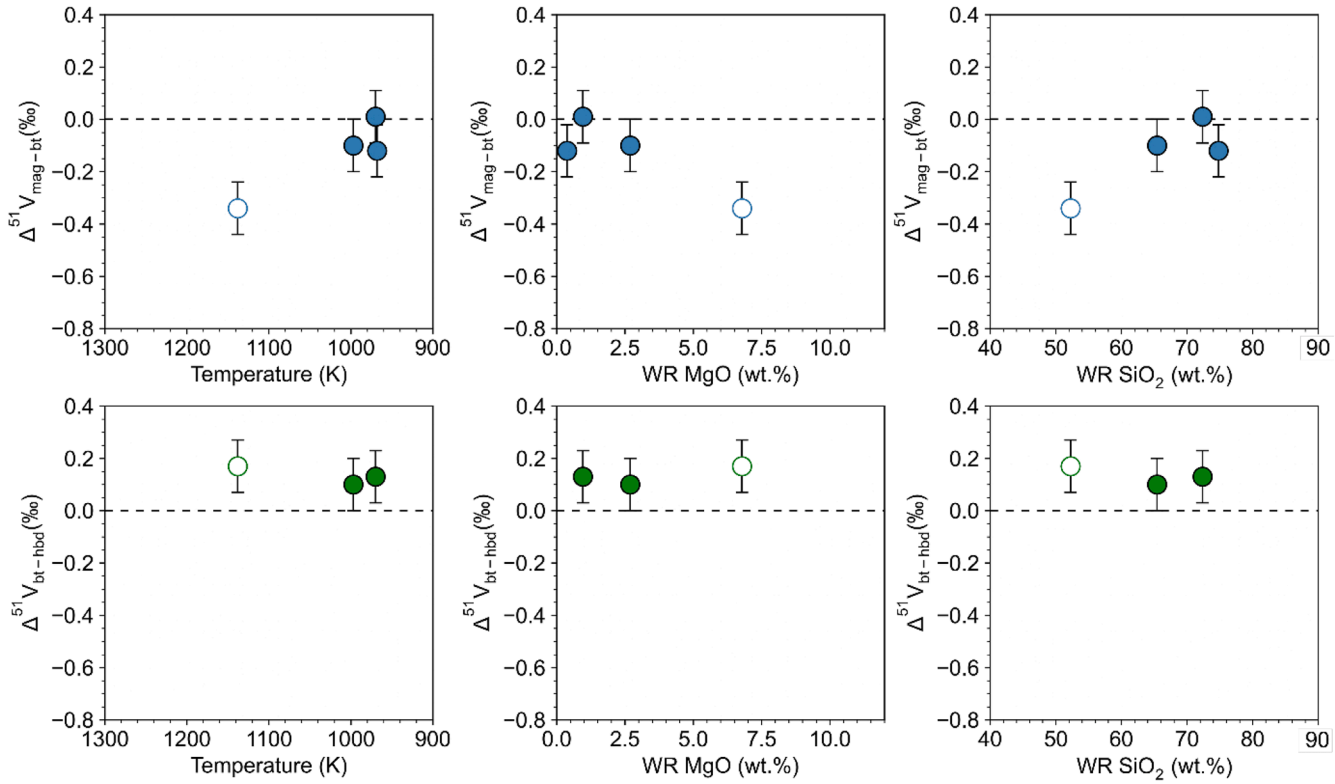

Fig. 3. Inter-mineral fractionation factors in the BPZP. Primocryst magnetite and biotite have V isotopic compositions within error in the same sample, and primocryst biotite is approximately 0.1 ‰ higher than coexisting hornblende. Whole rock SiO_2 and MgO data are from Wyborn (1983). Temperature values are from Stow et al. (2022). Minerals with interstitial morphologies are shown with open symbols, and primocrysts shown with filled symbols. Interstitial phases may not have crystallised in isotopic equilibrium based on textural observations of thin sections. Uncertainties are given as ± 0.1 ‰, which is the typical analytical uncertainty (2SD). The dashed line shows $\Delta^{51}V_{min\text{-}min} = 0$, i.e. when mineral separates have identical isotopic compositions.

log units, Sossi et al. (2018) predict a variation in $\Delta^{51}V_{mag\text{-}melt}$ of approximately 0.1 ‰. Since the BPZP is an intrusive system, we do not have a coexisting melt phase to analyse, so cannot directly compare $\Delta^{51}V_{min\text{-}melt}$ values. However, we can consider the magnetite mineral separates, which show a 0.6 ‰ range in $\delta^{51}V$ across the differentiation sequence. This range is much larger than the difference in $\Delta^{51}V_{mag\text{-}melt}$ predicted due to variation in magma fO_2, which highlights that although fO_2 variations may exert some influence on V isotope fractionation in the BPZP, it is not the primary control. Instead, the increase in $\delta^{51}V$ of magnetite most likely reflects the increasing $\delta^{51}V$ of the evolving melt following the fractional crystallisation and removal of isotopically light biotite, magnetite and hornblende. This interpretation is supported by the other chemical variations in magnetite and biotite, such as decreasing TiO_2, V and MgO concentrations (Fig. 4; Fig. S-2; Fig. S-3), which reflect the decreasing concentrations of these elements in the magma during fractional crystallisation.

It is also important to emphasise that WR $Fe^{3+}/\Sigma Fe$ in the BPZP does not represent the $Fe^{3+}/\Sigma Fe$ of an evolving magma, but rather the mineralogy of the sample and whether Fe is hosted primarily as Fe^{3+} or Fe^{2+} in the different mineral phases. The increase in WR $Fe^{3+}/\Sigma Fe$ in the BPZP is due to an increased proportion of Fe hosted in magnetite ($Fe^{3+}/\Sigma Fe \sim 0.66$) in the more evolved samples, which has a higher $Fe^{3+}/\Sigma Fe$ than silicate phases like pyroxene, biotite and hornblende ($Fe^{3+}/\Sigma Fe$ values of ~0, 0.12–0.22 and 0.18–0.25 respectively; Wyborn, 1983). Therefore, the correlation between magnetite $\delta^{51}V$ and WR $Fe^{3+}/\Sigma Fe$ in the BPZP does not indicate a relationship between $\delta^{51}V$ and magma redox state. Instead, variations in $\delta^{51}V$ and WR $Fe^{3+}/\Sigma Fe$ are due to fractional crystallisation and subsequent changes in the modal mineralogy of samples. This demonstrates that magnetite V isotopic composition cannot be easily used to track fO_2 variations in an individual pluton.

5.5. Effects of weathering on $\delta^{51}V$

We took care to sample unweathered material, and all WR samples have CIA values (Chemical Index of Alteration, after Nesbitt and Young, 1982) between 39 – 51 (Table S-2), typical of unweathered mafic and felsic rocks. Therefore, the mineral separates and whole rock samples from the BPZP show a large range in $\delta^{51}V$ caused only by primary magmatic processes, and provide a snapshot of the isotopic variability present in the unweathered crust. BPZP whole rock powders and mineral separates span a range in $\delta^{51}V_{AA}$ from −1.15 ± 0.04 ‰ (2SD) to −0.56 ± 0.06 ‰ (2SD) (Fig. 2). Compared to basaltic terranes, which thus far show $\delta^{51}V_{AA}$ values clustering around −0.8 ‰ to −1.0 ‰ (Prytulak et al., 2013, 2016; Wu et al., 2018; Qi et al., 2019; Ding et al., 2020; Novella et al., 2020; Stow et al., 2023), our new data show that the V isotopic composition of intermediate to felsic plutonic rocks, which make up the majority of the present day upper continental crust, could be highly variable, even before consideration of weathering induced isotopic fractionation.

The effects of chemical weathering on V isotopes are unclear. Latosols which have undergone high degrees of chemical weathering have indistinguishable $\delta^{51}V$ values compared to the unweathered bedrock (Qi et al., 2022). Although redox changes occur during the oxidation of V^{3+} and V^{4+} in primary minerals to V^{5+}, the lack of V isotope fractionation is explained by the congruent weathering of primary minerals and then quantitative sorption of V^{5+} onto Fe (oxyhydr)oxides (Qi et al., 2022). However, in lower intensity weathering regimes, it is likely that weathering reactions would not be congruent, and thus V isotope fractionation may be expected based on the different chemical weathering rates of specific silicate and oxide minerals (e.g. Brantley and Olsen, 2014). Given the range in $\delta^{51}V$ in primary magmatic minerals we observe in the BPZP, weathering processes could cause additional V

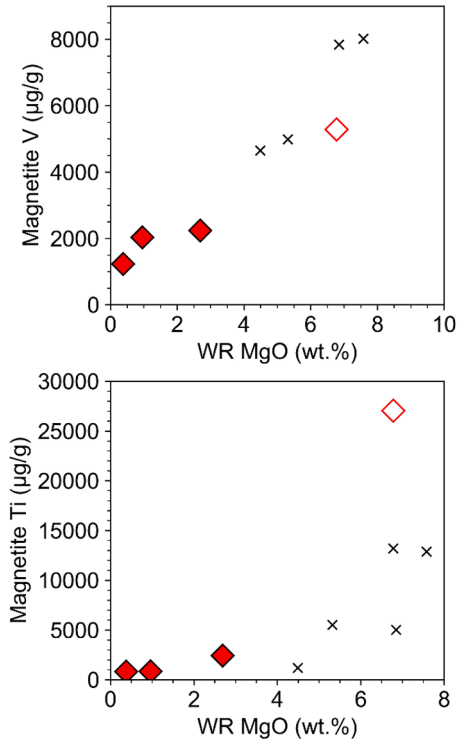

Fig. 4. Vanadium and titanium concentrations in magnetite measured by ICP-QQQ-MS. The BPZP samples are shown by the red diamonds. Interstitial magnetite is shown by open symbols, and primocrysts shown with filled symbols. WR MgO content is from Wyborn (1983). Errors are the within run RSD of an individual measurement of each sample, and are smaller than the size of the symbols. Magnetite V and Ti concentrations decrease during magmatic differentiation, and fall on a similar trend to data from a different set of BPZP samples measured using LA-ICP-MS by Park et al. (2013), shown by the grey crosses.

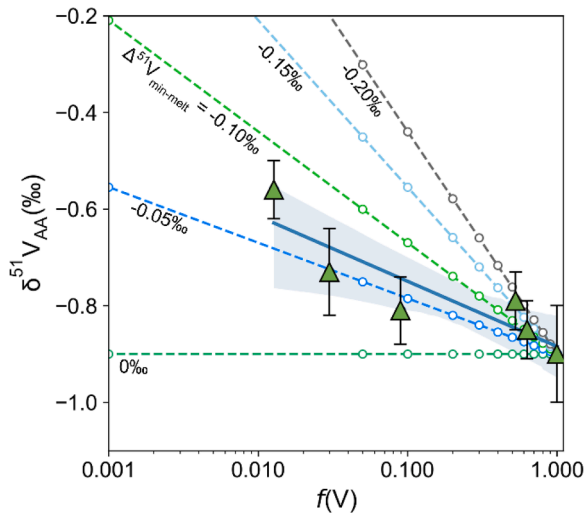

Fig. 5. The change in magma $\delta^{51}V$ during fractional crystallisation calculated using the Rayleigh equation: $\delta^{51}V = \delta^{51}V_{initial} + (\Delta^{51}V_{min\text{-}melt} \times \ln fV)$. The BPZP data is shown by the green triangles. For the samples, the fraction of V remaining (fV) is calculated by $f(V) = (F \times C)/C_{initial}$ where F is the melt fraction estimated from the change in incompatible element concentration (e.g. Rb, Th), and C is the melt V concentration. The BPZP data is best described by a bulk $\Delta^{51}V_{min\text{-}melt}$ value between −0.05 ‰ and −0.10 ‰.

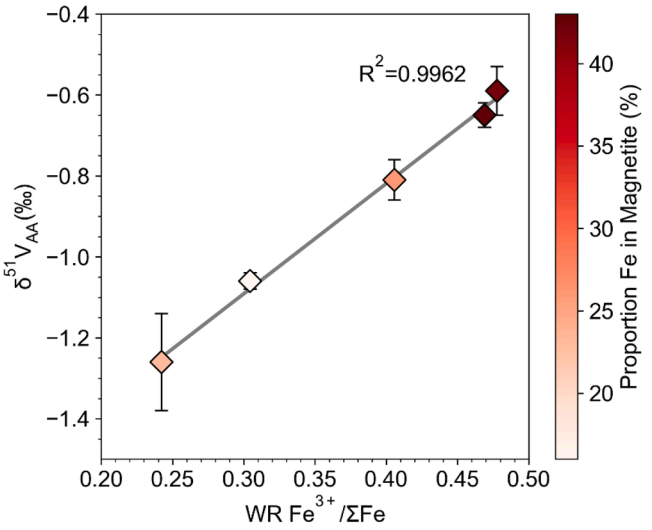

Fig. 6. Vanadium isotopic composition of magnetite mineral separates against WR $Fe^{3+}/\Sigma Fe$. The symbols are coloured based on the proportion of Fe in the whole rock sample hosted in the magnetite, calculated by mass balance. There is a strong positive correlation ($r^2 = 0.9962$) between magnetite $\delta^{51}V$ and WR $Fe^{3+}/\Sigma Fe$, however this does not demonstrate a simple relationship between $\delta^{51}V$ and magma redox state, because WR $Fe^{3+}/\Sigma Fe$ primarily reflects the mineralogy of the samples (see text for more details).

isotope variation in both the upper crust and the clastic sedimentary rocks eroded from it.

5.6. Secular variations in $\delta^{51}V$ in the continental crust

There are few geological archives available to investigate temporal variations in upper crustal composition. Recently, focus has centred on glacial diamictites as unique and informative samples, because the fine-grained sample matrix is composed of regolith and bedrock eroded from large areas of crust by glaciers and ice sheets, and thus can record an average crustal composition (e.g. Gaschnig et al., 2014). The diamictites of Gaschnig et al. (2014) have been well characterised for major and trace elements, and numerous stable isotope systems to date (e.g. Gaschnig et al., 2014, 2016; Li et al., 2016; Greaney et al., 2020; Klaver et al., 2021; Tian et al., 2021; Liu et al., 2022; Murphy et al., 2022; Saji et al., 2023), including vanadium (Tian et al., 2023).

Tian et al. (2023) demonstrated that the V isotopic composition of glacial diamictite composites increases through time from the Meso-archean to Palaeozoic. They interpret the temporal increase in diamictite $\delta^{51}V$ to reflect an increase in the proportion of felsic rocks in the upper continental crust since 3 Ga. The glacial diamictites display a range in $\delta^{51}V$ between -0.89 ± 0.03 ‰ (2SD) to -0.58 ± 0.04 ‰ (2SD) over this 3 Ga time period (Tian et al., 2023). This is smaller than the range in whole rock $\delta^{51}V$ that we observe across the single BPZP (WR $\delta^{51}V_{AA} = -1.15 \pm 0.04$ ‰ (2SD) to -0.56 ± 0.06 ‰ (2SD); Fig. 7), even though the diamictites and BPZP samples span a similar range in WR MgO content.

Using the V isotope data, Tian et al. (2023) determined that there was no felsic continental crust before 2.9 Ga, and minor (approximately 16%) felsic crust at 2.4 Ga. However, based on Ti isotope data from the same diamictite samples, Saji et al. (2023) calculated that a significant proportion of felsic crust (approximately 75%) was present at 2.9 Ga and 2.4 Ga. This discrepancy is surprising given that V and Ti isotopes are thought to behave similarly in magmatic systems. The V and Ti isotopic compositions of magmas increase during magmatic differentiation, and in both cases, this has been interpreted to be due to the fractional crystallisation and removal of isotopically light Fe-Ti oxides (e.g. Prytulak et al., 2016; Ding et al., 2020; Johnson et al., 2019; Hoare et al.,

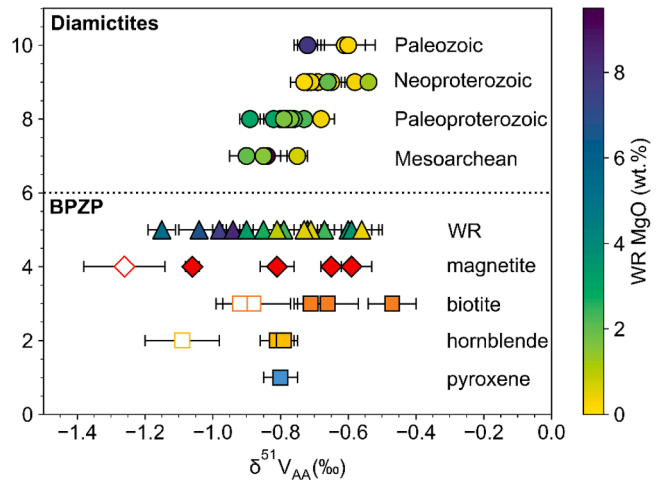

Fig. 7. Vanadium isotopic composition of glacial diamictites and whole rocks (WR) and mineral separates from the BPZP. The glacial diamictite data is from Tian et al. (2023). Error bars are as 2SD. The BPZP WR samples and diamictites are coloured based on WR MgO content, using concentrations from Wyborn (1983) and Tian et al. (2023) respectively. The BPZP WR and mineral separate data from an individual pluton spans a greater range in $\delta^{51}V$ than the glacial diamictites, despite spanning a similar range in WR MgO.

2022).

However, our study of the BPZP hints at differences between the behaviours of V and Ti isotopes in magmatic systems, which may help to explain some discrepancy between these two interpretations of crustal composition through time. Firstly, although it has previously been documented that Fe-Ti oxide fractionation is the main driver of V isotope fractionation, we demonstrate that silicate phases such as biotite and hornblende can be important hosts of V. This contrasts with the Ti isotope system, where Fe-Ti oxides are typically the dominant host of Ti (e.g. Hoare et al., 2022). Secondly, distinct oxide-melt fractionation factors are documented for Ti in magnetite, ilmenite and rutile, leading to contrasting Ti isotopic trends in calc-alkaline and tholeiitic settings (e.g. Hoare et al., 2022), but this has not yet been directly demonstrated for V isotopes using mineral separates. Together, this means that mafic and felsic end-members from different tectonic settings may have distinct isotopic compositions and thus influence these estimates of felsic crust proportion. Finally, the effects of weathering remain poorly constrained for both V and Ti isotopes (e.g. He et al., 2022; Qi et al., 2022), and the inherent variability in $\delta^{51}V$ observed in the BPZP driven only by magmatic differentiation highlights that weathering processes could potentially generate even more isotopic variability in the continental crust.

Future studies of crustal rocks are necessary to establish if the $\delta^{51}V$ variability in the BPZP is typical of calc-alkaline plutons and if a similar range in $\delta^{51}V$ is observed in tholeiitic plutons with different fractionating mineral assemblages. These studies will provide an important baseline for understanding V isotopic behaviour in simple intrusive settings, and open the door to using V isotopes as a tool to investigate more complex mush systems. In addition, combining work on plutonic rocks with studies on their weathering products will give us a greater understanding of the controls of V isotope fractionation and mass balance during the formation and alteration of the continental crust.

6. Conclusions

We report the first V isotope measurements of WR samples and mineral separates from a closed system, calc-alkaline intrusive suite, representative of typical upper continental crust.

1. The WR samples show a diffuse increase in $\delta^{51}V$ during differentiation but values are highly scattered, demonstrating the inherent heterogeneity encountered when analysing coarse grained intrusive samples.
2. The mineral separates show a well-defined increase in $\delta^{51}V$ during magmatic differentiation. In contrast to previous work which has suggested that Fe-Ti oxide crystallisation is the primary driver of increasing $\delta^{51}V$, we demonstrate that silicates such as biotite and hornblende are also important hosts of V.
3. Primocryst magnetite, biotite and hornblende have identical $\delta^{51}V$ in individual samples, because they all host predominantly VI-fold coordinated V^{3+}. V isotopic fractionation is dominantly controlled by the bonding environment of V in minerals and melt, rather than variations in fO_2. Therefore, V isotopes in mineral separates are likely not a straightforward redox proxy.
4. WR $\delta^{51}V_{AA}$ varies between -1.15 ± 0.04 ‰ (2SD) and -0.56 ± 0.06 ‰ (2SD) in a single pluton, which hints that the upper continental crust has extremely variable V isotopic composition over small areas.

CRediT authorship contribution statement

Madeleine A. Stow: Writing – review & editing, Writing – original draft, Visualization, Methodology, Investigation, Funding acquisition, Formal analysis, Conceptualization. **Julie Prytulak:** Writing – review & editing, Supervision, Resources, Methodology, Funding acquisition, Conceptualization. **Madeleine C.S. Humphreys:** Writing – review & editing, Supervision, Conceptualization. **Samantha J. Hammond:** Writing – review & editing, Methodology, Formal analysis. **Geoffrey M. Nowell:** Writing – review & editing, Supervision, Methodology.

Declaration of competing interest

The authors declare that they have no known competing financial interests or personal relationships that could have appeared to influence the work reported in this paper.

Data availability

All data presented in the study are available in the manuscript and supplementary materials.

Acknowledgements

This research was supported by a NERC IAPETUS Doctoral Training Programme (NE/L002590/1) studentship to MAS. Doone Wyborn and Hugh O'Neill are thanked for fieldwork assistance to Boggy Plain during JP's visit to ANU in 2013, funded by Australian Research Council Discovery Grant DP130101355 to H.St.C. O'Neill and JP. JP thanks Doone Wyborn and Bruce Chappell for many interesting discussions about granite petrogenesis during her 2013 visit. We think M.-A. Millet for comments on an earlier version of this work, reviews from R. Ickert and an anonymous reviewer, and editorial handling by F. Moynier, all of which improved the clarity of our study.

Supplementary materials

Supplementary material associated with this article can be found, in the online version, at doi:10.1016/j.epsl.2024.118825.

References

Bachmann, O., Bergantz, G.W., 2004. On the origin of crystal-poor rhyolites: extracted from batholithic crystal mushes. J. Petrol. 45, 1565–1582. https://doi.org/10.1093/petrology/egh019.

Brantley, S.L., Olsen, A.A., 2014. Reaction kinetics of primary rock-forming minerals under ambient conditions. In: Holland, H.D., Turekian, K.K. (Eds.), Treatise On Geochemistry, 2nd Edition. Elsevier, Oxford, pp. 69–113.

Brett, A., Prytulak, J., Hammond, S.J., Rehkämper, M., 2018. Thallium mass fraction and stable isotope ratios of sixteen geological reference materials. Geostand. Geoanalytical Res. 42, 339–360. https://doi.org/10.1111/ggr.12215.

Cao, Y., Wang, C.Y., Huang, F., Zhang, Z., 2019. Iron isotope systematics of the panzhihua mafic layered intrusion associated with giant Fe-Ti oxide deposit in the emeishan large igneous province, SW China. J. Geophys. Res. Solid Earth 124, 358–375. https://doi.org/10.1029/2018JB016466.

Chappell, B.W., Wyborn, D., 2004. Cumulate and cumulative granites and associated rocks. Resour. Geol. 54, 227–240. https://doi.org/10.1111/j.1751-3928.2004.tb00204.x.

Chen, L.-M., Song, X.-Y., Zhu, X.-K., Zhang, X.-Q., Yu, S.-Y., Yi, J.-N, 2014. Iron isotope fractionation during crystallization and sub-solidus re-equilibration: constraints from the Baima mafic layered intrusion, SW China. Chem. Geol. 380, 97–109. https://doi.org/10.1016/j.chemgeo.2014.04.020.

Chen, L.-M., Teng, F.-Z., Song, X.-Y., Luan, Y., Yu, S.-Y., Kang, J, 2021. Origins and implications of magnesium isotopic heterogeneity in Fe-Ti oxides in layered mafic intrusions. Geochim. Cosmochim. Acta 308, 273–290. https://doi.org/10.1016/j.gca.2021.06.016.

Ding, X., Helz, R.T., Qi, Y., Huang, F., 2020. Vanadium isotope fractionation during differentiation of Kilauea Iki lava lake, Hawaii. Geochim. Cosmochim. Acta 289, 114–129. https://doi.org/10.1016/j.gca.2020.08.023.

Dziony, W., Horn, I., Lattard, D., Koepke, J., Steinhoefel, G., Schuessler, J.A., Holtz, F., 2014. In-situ Fe isotope ratio determination in Fe–Ti oxides and sulfides from drilled gabbros and basalt from the IODP Hole 1256D in the eastern equatorial Pacific. Chem. Geol. 363, 101–113. https://doi.org/10.1016/j.chemgeo.2013.10.035.

Fan, H., Ostrander, C.M., Auro, M., Wen, H., Nielsen, S.G., 2021. Vanadium isotope evidence for expansive ocean Euxinia during the appearance of early Ediacara biota. Earth Planet Sci. Lett. 567, 117007 https://doi.org/10.1016/j.epsl.2021.117007.

Frost B.R. and Lindsley D.H. (1991) Occurrence of iron-titanium oxides in igneous rocks. In: Lindsley D. H. (Ed.), Oxide Minerals: Petrologic and Magnetic Significance, Reviews in Mineralogy and Geochemistry 25, pp. 433–468.

Gaschnig, R.M., Rudnick, R.L., McDonough, W.F., Kaufman, A.J., Hu, Z., Gao, S., 2014. Onset of oxidative weathering of continents recorded in the geochemistry of ancient glacial diamictites. Earth Planet Sci. Lett. 408, 87–99. https://doi.org/10.1016/j.epsl.2014.10.002.

Gaschnig, R.M., Rudnick, R.L., McDonough, W.F., Kaufman, A.J., Valley, J.W., Hu, Z., Gao, S., Beck, M.L., 2016. Compositional evolution of the upper continental crust through time, as constrained by ancient glacial diamictites. Geochim. Cosmochim. Acta 186, 316–343. https://doi.org/10.1016/j.gca.2016.03.020.

Giuli, G., Paris, E., Mungall, J., Romano, C., Dingwell, D., 2004. V oxidation state and coordination number in silicate glasses by XAS. Am. Mineral. 89, 1640–1646. https://doi.org/10.2138/am-2004-11-1208.

Greaney, A.T., Rudnick, R.L., Romaniello, S.J., Johnson, A.C., Gaschnig, R.M., Anbar, A.D., 2020. Molybdenum isotope fractionation in glacial diamictites tracks the onset of oxidative weathering of the continental crust. Earth Planet Sci. Lett. 534, 116083 https://doi.org/10.1016/j.epsl.2020.116083.

He, X., Ma, J., Wei, G., Wang, Z., Zhang, L., Zeng, Ti., Zhang, Z., 2022. Mass-dependent fractionation of titanium stable isotopes during intensive weathering of basalts. Earth Planet Sci. Lett. 579, 117347 https://doi.org/10.1016/j.epsl.2021.117347.

Hoare, L., Klaver, M., Muir, D.D., Klemme, S., Barling, J., Parkinson, I.J., Lissenberg, C.J., Millet, M.-A., 2022. Empirical and experimental constraints on Fe-Ti oxide-melt titanium isotope fractionation factors. Geochim. Cosmochim. Acta. 326, 253–272. https://doi.org/10.1016/j.gca.2022.02.011.

Holness, M.B., 2018. Melt segregation from silicic crystal mushes: a critical appraisal of possible mechanisms and their microstructural record. Contrib. Mineral Petrol. 173, 48. https://doi.org/10.1007/s00410-018-1465-2.

Hoskin, P.W.O., Kinny, P.D., Wyborn, D., Chappell, B.W., 2000. Identifying accessory mineral saturation during differentiation in granitoid magmas: an integrated approach. J. Petrol. 41, 1365–1396. https://doi.org/10.1093/petrology/41.9.1365.

Huang, J.H., Huang, F., Evans, L., Glasauer, S., 2015. Vanadium: global (bio) geochemistry. Chem. Geol. 417, 68–89. https://doi.org/10.1016/j.chemgeo.2015.09.019.

Huang, Y., Long, Z., Zhou, D., Wang, L., He, P., Zhang, G., Hughes, S.S., Yu, H., Huang, F., 2021. Fingerprinting vanadium in soils based on speciation characteristics and isotope compositions. Sci. Total Environ. 791, 148240 https://doi.org/10.1016/j.scitotenv.2021.148240.

Ickert, R.B., 2010. U-Pb, Lu-Hf, and O isotope Systematics of Zircon from Southeastern Australian Siluro-Devonian Granites. Australian National University. Ph. D. thesis.

Ickert, R.B., Williams, I.S., Wyborn, D., 2011. Ti in zircon from the Boggy Plain zoned pluton: implications for zircon petrology and Hadean tectonics. Contrib. Mineral Petrol. 162, 447–461. https://doi.org/10.1007/s00410-010-0605-0.

Johnson, A.C., Aarons, S.M., Dauphas, N., Nie, N.X., Zeng, H., Helz, R.T., Romaniello, S.J., Anbar, A.D., 2019. Titanium isotopic fractionation in Kilauea Iki lava lake driven by oxide crystallization. Geochim. Cosmochim. Acta 264, 180–190. https://doi.org/10.1016/j.gca.2019.08.022.

Klaver, M., MacLennan, S.A., Ibañez-Mejia, M., Tissot, F.L.H., Vroon, P.Z., Millet, M.A., 2021. Reliability of detrital marine sediments as proxy for continental crust composition: the effects of hydrodynamic sorting on Ti and Zr isotope systematics. Geochim. Cosmochim. Acta 310, 221–239. https://doi.org/10.1016/j.gca.2021.05.030.

Li, S., Gaschnig, R.M., Rudnick, R.L., 2016. Insights into chemical weathering of the upper continental crust from the geochemistry of ancient glacial diamictites. Geochim. Cosmochim. Acta 176, 96–117. https://doi.org/10.1016/j.gca.2015.12.012.

Liu, X.-M., Gaschnig, R.M., Rudnick, R.L., Hazen, R.M., Shahar, A., 2022. Constant iron isotope composition of the upper continental crust over the past 3 Gyr. Geochem. Persp. Let. 22, 16–19. https://doi.org/10.7185/geochemlet.2221.

Murphy, M.E., Savage, P.S., Gardiner, N.J., Prave, A.R., Gaschnig, R.M., Rudnick, R.L., 2022. Homogenising the upper continental crust: the Si isotope evolution of the crust recorded by ancient glacial diamictites. Earth Planet Sci. Lett. 591, 117620 https://doi.org/10.1016/j.epsl.2022.117620.

Nesbitt, H.W., Young, G.M., 1982. Early Proterozoic climates and plate motions inferred from major element chemistry of lutites. Nature 299, 715–717. https://doi.org/10.1038/299715a0.

Nie, N.X., Dauphas, N., Alp, E.E., Zeng, H., Sio, C.K., Hu, J.Y., Chen, X., Aarons, S.M., Zhang, Z., Tian, H.-C., Wang, D., Prissel, K.B., Greer, J., Bi, W., Hu, M.Y., Zhao, J., Shahar, A., Roskosz, M., Teng, F.-Z., Krawczynski, M.J., Heck, P.R., Spear, F.S., 2021. Iron, magnesium, and titanium isotopic fractionations between garnet, ilmenite, fayalite, biotite, and tourmaline: results from NRIXS, ab initio, and study of mineral separates from the Moosilauke metapelite. Geochim. Cosmochim. Acta 302, 18–45. https://doi.org/10.1016/j.gca.2021.03.014.

Nielsen, S.G., Prytulak, J., Halliday, A.N., 2011. Determination of precise and accurate 51V/50V isotope ratios by MC-ICP-MS, part 1: chemical separation of vanadium and mass spectrometric protocols. Geostand. Geoanalytical Res. 35, 293–306. https://doi.org/10.1111/j.1751-908X.2011.00106.x.

Novella, D., Maclennan, J., Shorttle, O., Prytulak, J., Murton, B.J., 2020. A multi-proxy investigation of mantle oxygen fugacity along the Reykjanes Ridge. Earth Planet Sci. Lett. 531, 115973 https://doi.org/10.1016/j.epsl.2019.115973.

O'Neill, H.S.C., Navrotsky, A., 1984. Cation distributions and thermodynamic properties of binary spinel solid solutions. Am. Mineral 69, 733–753.

Park, J.W., Campbell, I.H., Ickert, R.B., Allen, C.M., 2013. Chalcophile element geochemistry of the Boggy Plain zoned pluton, southeastern Australia: a S-saturated barren compositionally diverse magmatic system. Contrib. Mineral Petrol. 165, 217–236. https://doi.org/10.1007/s00410-012-0806-9.

Prytulak, J., Sossi, P.A., Halliday, A.N., Plank, T., Savage, P.S., Woodhead, J.D., 2016. Stable vanadium isotopes as a redox proxy in magmatic systems? Geochem. Persp. Let. 3, 75–84. https://doi.org/10.7185/geochemlet.1708.

Prytulak, J., Nielsen, S.G., Ionov, D.A., Halliday, A.N., Harvey, J., Kelley, K.A., Niu, Y.L., Peate, D.W., Shimizu, K., Sims, K.W.W., 2013. The stable vanadium isotope composition of the mantle and mafic lavas. Earth Planet Sci. Lett. 365, 177–189. https://doi.org/10.1016/j.epsl.2013.01.010.

Prytulak, J., Nielsen, S.G., Halliday, A.N., 2011. Determination of precise and accurate 51V/50V isotope ratios by multi-collector ICP-MS, part 2: isotopic composition of six reference materials plus the allende chondrite and verification tests. Geostand. Geoanalytical Res. 35, 307–318. https://doi.org/10.1111/j.1751-908X.2011.00105.x.

Qi, Y.-H., Wu, F., Ionov, D.A., Puchtel, I.S., Carlson, R.W., Nicklas, R.W., Yu, H.M., Kang, J.T., Li, C.H., Huang, F., 2019. Vanadium isotope composition of the Bulk Silicate Earth: constraints from peridotites and komatiites. Geochim. Cosmochim. Acta 259, 288–301. https://doi.org/10.1016/j.gca.2019.06.008.

Qi, Y.-H., Gong, Y.-Z., Wu, F., Lu, Y., Cheng, W., Huang, F., Yu, H.-M, 2022. Coupled variations in V-Fe abundances and isotope compositions in latosols: implications for V mobilization during chemical weathering. Geochim. Cosmochim. Acta 320, 26–40. https://doi.org/10.1016/j.gca.2021.12.028.

Rabin, S., Blanchard, M., Pinilla, C., Poitrasson, F., Gregoire, M., 2021. First-principles calculation of iron and silicon isotope fractionation between Fe-bearing minerals at magmatic temperatures: the importance of second atomic neighbors. Geochim. Cosmochim. Acta 304, 101–118. https://doi.org/10.1016/j.gca.2021.03.028.

Redhammer, G.J., Roth, G., 2002. Crystal structure and Mössbauer spectroscopy of the synthetic amphibole potassic-ferri-ferrorichterite at 298 K and low temperatures (80-110 K). Eur. J. Miner. 14, 105–114. https://doi.org/10.1127/0935-1221/2002/0014-0105.

Righter, K., Sutton, S.R., Newville, M., Le, L., Schwandt, C.S., Uchida, H., Lavina, B., Downs, R.T., 2006. An experimental study of the oxidation state of vanadium in spinel and basaltic melt with implications for the origin of planetary basalt. Am. Mineral 91, 1643–1656. https://doi.org/10.2138/am.2006.2111.

Rudnick, R.L., Gao, S., 2014. Composition of the Continental Crust. In: Holland, H.D., Turekian, K.K. (Eds.), Treatise On Geochemistry, 2nd Edition. Elsevier, Oxford, pp. 1–51.

Saji, N.S., Rudnick, R.L., Gaschnig, R.M., Millet, M.-A., 2023. Titanium isotope evidence for the high topography of Nuna and Gondwana – implications for earth's redox and biological evolution. Earth Planet Sci. Lett. 615, 118214 https://doi.org/10.1016/j.epsl.2023.118214.

Schauble, E.A., 2004. Applying stable isotope fractionation theory to new systems. Rev. Mineral. Geochem. 55, 65–111. https://doi.org/10.2138/gsrmg.55.1.65.

Schuth, S., Brüske, A., Hohl, S.V., Jiang, S.Y., Meinhardt, A.K., Gregory, D.D., Viehmann, S., Weyer, S., 2019. Vanadium and its isotope composition of river water and seawater: analytical improvement and implications for vanadium isotope fractionation. Chem. Geol. 528, 119261 https://doi.org/10.1016/j.chemgeo.2019.07.036.

Shannon, R.D., 1976. Revised effective ionic radii and systematic studies of interatomic distances in halides and chalcogenides. Acta Crystallogr. Sect. A 32, 751–767. https://doi.org/10.1107/S0567739476001551.

Shiller, A.M., Mao, L., 2000. Dissolved vanadium in rivers: effects of silicate weathering. Chem. Geol. 165, 13–22. https://doi.org/10.1016/S0009-2541(99)00160-6.

Sossi, P.A., O'Neill, H.S.C, 2017. The effect of bonding environment on iron isotope fractionation between minerals at high temperature. Geochim. Cosmochim. Acta 196, 121–143. https://doi.org/10.1016/j.gca.2016.09.017.

Sossi, P.A., Prytulak, J., O'Neill, H.S.C, 2018. Experimental calibration of vanadium partitioning and stable isotope fractionation between hydrous granitic melt and magnetite at 800°C and 0.5 GPa. Contrib. Mineral Petrol. 173, 27. https://doi.org/10.1007/s00410-018-1451-8.

Stow, M.A., Prytulak, J., Humphreys, M.C.S., Nowell, G.M., 2022. Integrated petrological and Fe-Zn isotopic modelling of plutonic differentiation. Geochim. Cosmochim. Acta 320, 366–391. https://doi.org/10.1016/j.gca.2021.12.018.

Stow, M.A., Prytulak, J., Burton, K.W., Nowell, G.M., Marshall, E.W., Halldórsson, S.A., Matthews, S., Rasmussen, M.B., Ranta, E., Caracciolo, A., 2023. No V-Fe-Zn isotopic variation in basalts from the 2021 Fagradalsfjall eruption. Geochem. Persp. Let. 27, 54–58. https://doi.org/10.7185/geochemlet.2335.

Sutton, S.R., Karner, J., Papike, J., Delaney, J.S., Shearer, C., Newville, M., Eng, P., Rivers, M., Dyar, M.D., 2005. Vanadium K edge XANES of synthetic and natural basaltic glasses and application to microscale oxygen barometry. Geochim. Cosmochim. Acta 69, 2333–2348. https://doi.org/10.1016/j.gca.2004.10.013.

Tian, S., Ding, X., Qi, Y., Wu, F., Cai, Y., Gaschnig, R.M., Xiao, Z., Lv, W., Rudnick, R.L., Huang, F., 2023. Dominance of felsic continental crust on Earth after 3 billion years ago is recorded by vanadium isotopes. Proc. Natl. Acad. Sci. 120, e2220563120 https://doi.org/10.1073/pnas.2220563120.

Tian, S., Moynier, F., Inglis, E.C., Rudnick, R.L., Huang, F., Chauvel, C., Creech, J.B., Gaschnig, R.M., Wang, Z., Guo, J.L., 2021. Zirconium isotopic composition of the upper continental crust through time. Earth Planet Sci. Lett. 572, 117086 https://doi.org/10.1016/j.epsl.2021.117086.

Toplis, M.J., Corgne, A., 2002. An experimental study of element partitioning between magnetite, clinopyroxene and iron-bearing silicate liquids with particular emphasis on vanadium. Contrib. Mineral Petrol. 144, 22–37. https://doi.org/10.1007/s00410-002-0382-5.

Wei, F., Prytulak, J., Xu, J., Wei, W., Hammond, J.O.S., Zhao, B., 2017. The cause and source of melting for the most recent volcanism in Tibet: a combined geochemical and geophysical perspective. Lithos 288–289, 175–190. https://doi.org/10.1016/j.lithos.2017.07.003.

Wei, W., Chen, X., Ling, H.F., Wu, F., Dong, L.H., Pan, S., Jing, Z., Huang, F., 2023. Vanadium isotope evidence for widespread marine oxygenation from the late Ediacaran to early Cambrian. Earth Planet Sci. Lett. 602, 117942 https://doi.org/10.1016/j.epsl.2022.117942.

Wu, F., Owens, J.D., Huang, T., Sarafian, A., Huang, K.-F., Sen, I.S., Horner, T.J., Blusztajn, J., Morton, P., Nielsen, S.G., 2019. Vanadium isotope composition of seawater. Geochim. Cosmochim. Acta 244, 403–415. https://doi.org/10.1016/j.gca.2018.10.010.

Wu, F., Qi, Y., Perfit, M.R., Gao, Y., Langmuir, C.H., Wanless, V.D., Yu, H., Huang, F., 2018. Vanadium isotope compositions of mid-ocean ridge lavas and altered oceanic crust. Earth Planet Sci. Lett. 493, 128–139. https://doi.org/10.1016/j.epsl.2018.04.009.

Wu, F., Qi, Y., Yu, H., Tian, S., Hou, Z., Huang, F., 2016. Vanadium isotope measurement by MC-ICP-MS. Chem. Geol. 421, 17–25. https://doi.org/10.1016/j.chemgeo.2015.11.027.

Wu, F., Qin, T., Li, X., Liu, Y., Huang, J.H., Wu, Z., Huang, F., 2015. First-principles investigation of vanadium isotope fractionation in solution and during adsorption. Earth Planet Sci. Lett. 426, 216–224. https://doi.org/10.1016/j.epsl.2015.06.048.

Wu, F., Owens, J.D., Scholz, F., Huang, L., Li, S., Riedinger, N., Peterson, L.C., German, C. R., Nielsen, S.G., 2020. Sedimentary vanadium isotope signatures in low oxygen marine conditions. Geochim. Cosmochim. Acta 284, 134–155. https://doi.org/10.1016/j.gca.2020.06.013.

Wyborn, D., Chappell, B.W., James, M., 2001. Examples of convective fractionation in high-temperature granites from the Lachlan fold belt. Aust. J. Earth Sci. 48, 531–541. https://doi.org/10.1046/j.1440-0952.2001.00877.x.

Wyborn, D., Turner, B.S., Chappell, B.W., 1987. The boggy plain supersuite: a distinctive belt of I-type igneous rocks of potential economic significance in the Lachlan fold belt. Aust. J. Earth Sci. 34, 21–43. https://doi.org/10.1080/08120098708729392.

Wyborn, D., 1983. Fractionation Processes in the Boggy Plain Zoned Pluton. Australian National University. PhD Thesis.